



[Journal of Geophysical Research Oceans]

Supporting Information for

[Contribution of biological effects to carbonate-system variations and the air-water CO₂ flux in inner and outer bays in Japan]

Tatsuki Tokoro^{*1,2}, Shin-ichiro Nakaoka¹, Shintaro Takao¹, Tomohiro Kuwae², Atsushi Kubo³, Toru Endo⁴, Yukihiro Nojiri^{1,5}

¹Center for Global Environmental Research, National Institute for Environmental Studies, Tsukuba, Japan

²Coastal and Estuarine Environment Research Group, Port and Airport Research Institute, Yokosuka, Japan

³Department of Geosciences, Shizuoka University, Shizuoka, Japan

⁴Graduate School of Engineering, Osaka City University, Osaka, Japan

⁵Graduate School of Science and Technology, Hirosaki University, Hirosaki, Japan

Contents of this file

Text S1 to S3

Figures S1 to S4

Tables S1 to S2

References

Introduction

This supporting information contains: (1) a detailed description of the changepoint analysis for determining the upper limit of the distance parameter *dist* which is defined by Eq. [3]. (2) a detailed description of the uncertainty of riverine endmember dissolved inorganic carbon (DIC) (3) a detailed description of the random error and the error associated with the uncertainty of the riverine endmember DIC.

Text S1. Changepoint analysis

The upper limit of the distance parameter *dist* was determined using changepoint analysis of the salinity and DIC, which are conservative parameters and should be unaffected by water temperature and salinity. The analysis focused on the rapid change of the variance of these parameters with *dist*, given the seasonal variability, and used the following equation (Lavielle, 2004):

$$J_n = m \log(\hat{\sigma}_{1:m}^2) + (n - m + 1) \log(\hat{\sigma}_{m+1:n}^2) \quad (\text{S1})$$

where n is the number of the salinity or DIC binned into 1-km *dist* intervals and m is the location of the change point ($1 < m < n$). $\hat{\sigma}_{i:j}^2$ is the variance of the data between i and j ($1 \leq i < j \leq n$). The change point m is determined in order to minimize the parameter J_n .

The change points for the salinity and DIC were 71 and 66 km in Tokyo Bay, 64 and 62 km in Ise Bay, and 33 and 48 km in Osaka Bay, respectively. In other words, the salinity and DIC in the bays at a distance more than 71 km from the head of the bay were relatively constant compared to the inner areas of the bays. We defined the range of the combined inner and outer bays in this study to be 90 km, to provide a conservative range, and the water between 90 km and 100 km was defined as the oceanic endmember. Data from more than 100 km from land was filtered out and not used in this study.

Text S2. Range of riverine endmember DIC

The range of riverine endmember DIC was estimated using the fugacity of CO₂ (fCO₂). Although riverine fCO₂ is variable because of the low buffering capacity, the

upper range should be limited because high water $f\text{CO}_2$ results in a strong CO_2 efflux to the atmosphere, which reduces the $f\text{CO}_2$ in water with low buffering capacity. Given previous information about riverine $f\text{CO}_2$ (Aufdenkamp et al., 2011; Chen and Borges, 2009), we set the range of $f\text{CO}_2$ as 100 to 10,000 μatm . From this, the respective upper and lower limits of riverine DIC were 1397.5 and 982.3 $\mu\text{mol kg}^{-1}$ in Tokyo Bay (1161.8 $\mu\text{mol kg}^{-1}$ from Eq. [3]), 909.8 and 513.3 $\mu\text{mol kg}^{-1}$ in Ise Bay (675.3 $\mu\text{mol kg}^{-1}$), and 1150.7 and 746.1 $\mu\text{mol kg}^{-1}$ in Osaka Bay (852.3 $\mu\text{mol kg}^{-1}$). Note that the equilibrium calculation uses the dissociation constant of carbonic acid provided by Millero (1979) because this constant is optimized for the calculation in freshwater. According to these estimates, we set $\pm 200 \mu\text{mol kg}^{-1}$ as the range of riverine endmember DIC, which satisfies the $f\text{CO}_2$ range.

Text S3. Error estimation

The calculation errors in this study were caused by 1) the measurement error of salinity and $f\text{CO}_2$, 2) error in total alkalinity (TA) as estimated from the empirical equation, 3) errors in the CO_2 flux calculation from the Eq [5] for the gas transfer velocity, and 4) the error from the imprecision in the range of the riverine endmember DIC. The propagation of error was calculated according to the procedure for estimating the abiotic CO_2 flux (F_{ab}) and the biotic CO_2 flux (F_b) (Figure 2). The error from the first three factors above resulted in the random error of the propagated parameters (“random error”) whereas the error from the last factor was estimated as the range of the parameters for cases with the upper and lower values for the range of the riverine DIC (“riverine error”). Because the random and riverine errors became large for the data from near-shore areas, we applied a constant random error to the averaged or binned parameters in order to avoid temporal and spatial inhomogeneity. The results of applying the constant random error and the mean of the riverine error are shown in Table S2.

First, the measurement errors of the National Institute for Environmental Studies (NIES) salinity and DIC were estimated as 0.005 and 0.5 μatm , respectively (Nakaoka et al., 2013). The errors for the corresponding Tokyo University of Marine Science and Technology (TUMSAT) data were about 0.3 (1%) and 0.4 μatm , respectively (Kubo et al., 2017), and about 0.03 (0.05 mS cm^{-1}) for Osaka City University (OCU) salinity. Note that OCU did not directly measure $f\text{CO}_2$. For ease of calculation, the $f\text{CO}_2$ error was assumed to be a uniform 0.5 μatm in this study.

The TA error from the empirical equation was defined as the standard deviation of the residuals of the empirical equation (34, 21 and 35 $\mu\text{mol kg}^{-1}$ for Tokyo Bay, Ise Bay and Osaka Bay, respectively) (Taguchi et al., 2009). Because these values were larger than the TA error caused by the salinity measurement error (1.8, 11, and 1.3 $\mu\text{mol kg}^{-1}$ for the data from NIES, TUMSAT and OCU, respectively), the random error of TA was determined only from the error of the empirical equation in this study.

The random error of DIC cannot be estimated by simple propagation because the carbonate equilibrium is calculated non-linearly. Therefore, the error was calculated using the asymptotic slope as follows:

$$Er_{-ob} = \left\{ \left[\left(\frac{\partial ob}{\partial Ex_1} \right) \cdot Er_{-Ex_1} \right]^2 + \left[\left(\frac{\partial ob}{\partial Ex_2} \right) \cdot Er_{-Ex_2} \right]^2 \right\}^{0.5} \quad (S2)$$

where Ob and Ex are the objective and explanatory variables, respectively. Er_{-ob} and Er_{-Ex_1} and Er_{-Ex_2} are the error of Ob and Ex, respectively. Here, Ob, Ex_1 and Ex_2 are the DIC, $f\text{CO}_2$ and TA, respectively. The partial differential of Ob and Ex (slope of the asymptote) was calculated using the water temperature, salinity, TA and DIC for each sampling point and date.

The random error of DIC_{ab} was calculated according to equation (3):

$$Er_{-DICab} = \left\{ \left(\frac{Sal}{Sal_o} Er_{-DICo} \right)^2 + \left[\frac{(Sal_o - Sal)}{Sal_o} Er_{-DICr} \right]^2 \right\}^{0.5} \quad (S3)$$

where Sal and Sal_o are the salinity of the data and the oceanic endmember for the month, respectively. Er_{-DICo} and Er_{-DICr} are the errors of oceanic and riverine endmember DICs, respectively. The former was calculated as the propagation of the DIC error used for the calculation of DIC_o in each month and equals the DIC error divided by the root square of the number of data. The latter was set to zero because the error was estimated separately as described below. Indeed, the random error of DIC_{ab} was relatively small (about 1 $\mu\text{mol kg}^{-1}$) compared to the error of DIC.

The calculation using equation (S2) was also applied for the calculation of $f\text{CO}_{2ab}$ error. In this case, Ob, Ex_1 and Ex_2 in equation (S2) are $f\text{CO}_{2ab}$, DIC_{ab} and TA, respectively. In addition, the error of CO_2 fluxes (F , F_{ab} , F_b) was calculated using the error of $f\text{CO}_2$ ($f\text{CO}_2$, $f\text{CO}_{2ab}$, $f\text{CO}_{2b}$) and the error of the gas transfer velocity (20%; Wanninkhof, 2014). The error of the solubility was neglected in this study because the effect was small (<1%) compared with the errors estimated above.

The riverine DIC error was calculated as the range of the results using the upper (+200 $\mu\text{mol kg}^{-1}$) and lower ($-200 \mu\text{mol kg}^{-1}$) values for the range of riverine DIC in each bay. Because the random error of the abiotic and biotic parameters depends on each parameter itself, the random error was estimated for both cases with upper and lower riverine DIC.

Because the random and riverine errors become large for data with low salinity, the weighted averaging of the different errors for analyzing the temporal and spatial variation should underestimate the contribution of the biological activities in near-shore areas. Therefore, we estimated a constant random error for each bay to avoid temporal and spatial inhomogeneity. In this study, the random error was interpolated to the 1-km dist \times 0.1-monthly data grid by the natural neighbor method, and the third quartile (75th percentile) was defined as the representative constant error for each bay. The error of an interpolated parameter was estimated as follows:

$$Er_{int_u} = \left(\frac{Er_{const_u}^2 + Er_{const}^2}{nd^{0.5}} \right)^{0.5} + \left[(\overline{P}_u - \overline{P})^2 \right]^{0.5}$$

$$Er_{int_l} = \left(\frac{Er_{const}^2 + Er_{const_l}^2}{nd^{0.5}} \right)^{0.5} + \left[(\overline{P} - \overline{P}_l)^2 \right]^{0.5} \quad (S4)$$

where Er_{int_u} and Er_{int_l} are the errors of the interpolated parameter for the cases with the upper and lower riverine DIC, respectively. The upper riverine DIC results in a positive and negative range for abiotic and biotic parameters, respectively, and vice versa. Er_{const} , Er_{const_u} , and Er_{const_l} are the constant errors in cases with the intermediate (the result of equation [3]), upper (+200 $\mu\text{mol kg}^{-1}$) and lower ($-200 \mu\text{mol kg}^{-1}$) riverine DIC. P , P_u and P_l are the interpolated parameters for the same cases of riverine DIC. The overbar indicates averaging or binning of the parameter. The term “nd” is the number of data for the averaging or binning under the assumption that the measurement data were distributed homogeneously; nd equals the number of data for each bay divided by the dist-monthly data grid (100×120) number used for the averaging. For example, if the monthly-binned average is calculated for Tokyo Bay, $nd = 18,118/(12,000/12)$.

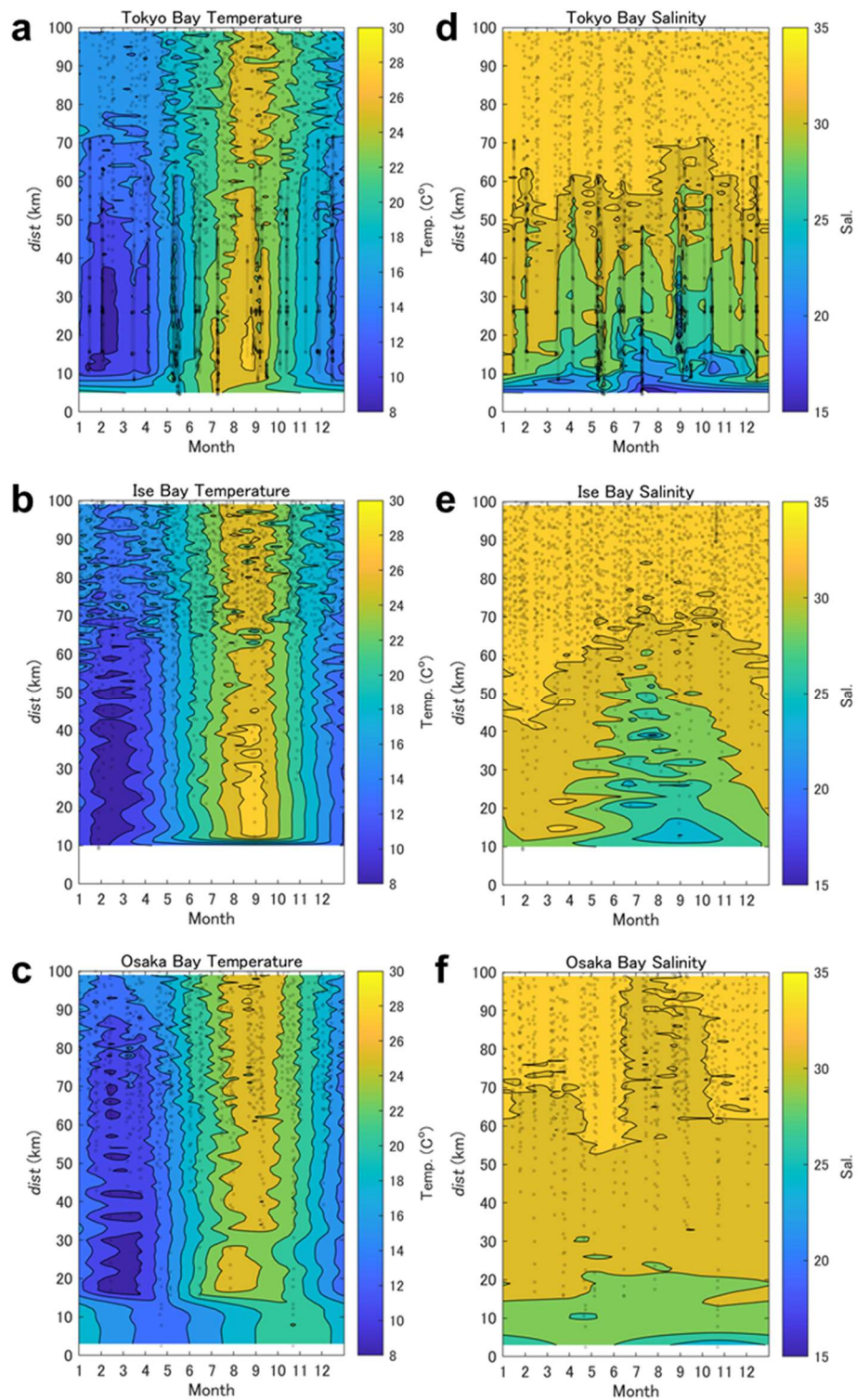


Figure S1. Temporal and spatial distributions of water temperature ((a): Tokyo Bay, (b): Ise Bay, (c): Osaka Bay) and salinity ((d): Tokyo Bay, (e): Ise Bay, (f): Osaka Bay). The color indicates the interpolated $0.1\text{-month} \times 1\text{-km}$ grid value. The gray dots show the distribution of direct measurements. The parameter *dist* represents the distance from a zero point in the mouth of the main river feeding the

inner bay (equation [1] in the main text).

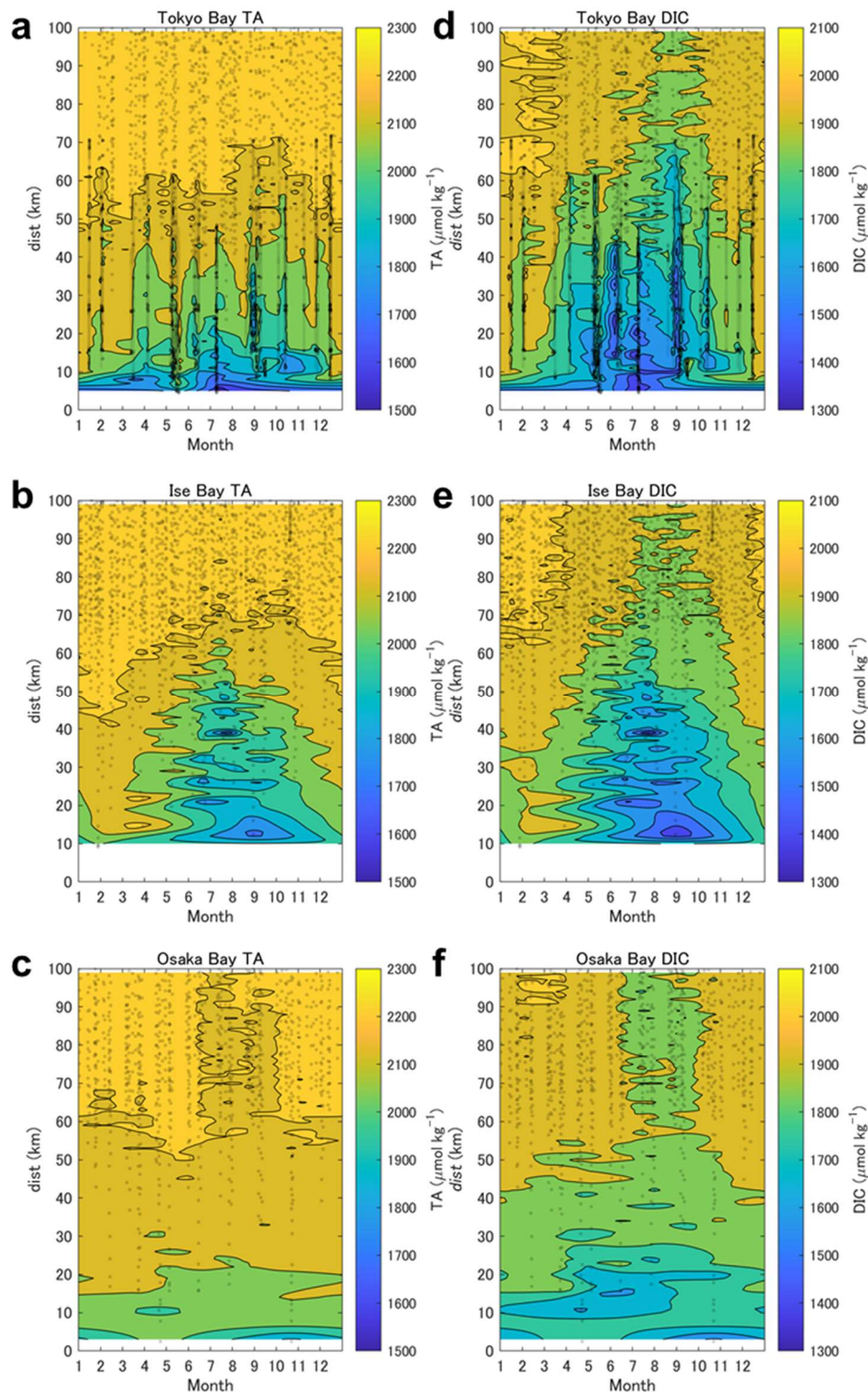


Figure S2. Temporal and spatial distributions of TA ((a): Tokyo Bay, (b): Ise Bay, (c): Osaka Bay) and DIC ((d): Tokyo Bay, (e): Ise Bay, (f): Osaka Bay). The colors and dots are as defined in Figure S1. The parameter *dist* represents the distance from a zero point in the mouth of the main river feeding the inner bay (equation [1] in the main text).

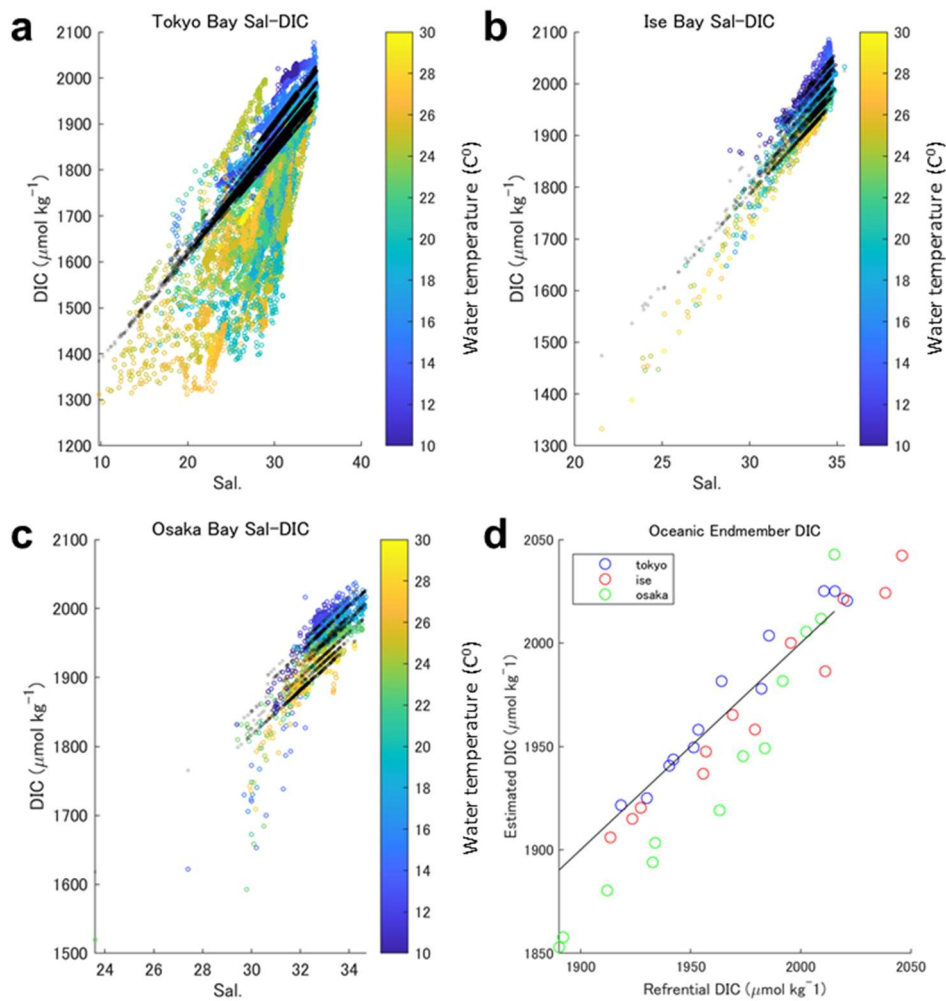


Figure S3. The relationships between salinity and DIC in (a) Tokyo, (b) Ise, and (c) Osaka Bays. The black dots are the interpolated values between the oceanic and riverine endmembers and defined as DIC_{ab} for each month. The graph in (d) shows a comparison between the DIC predicted using the empirical equation from a previous study for the value in the Kuroshio stream area (Ishii et al., 2011) and the estimated DIC of oceanic endmembers in this study. The black line in this graph shows $y = x$.

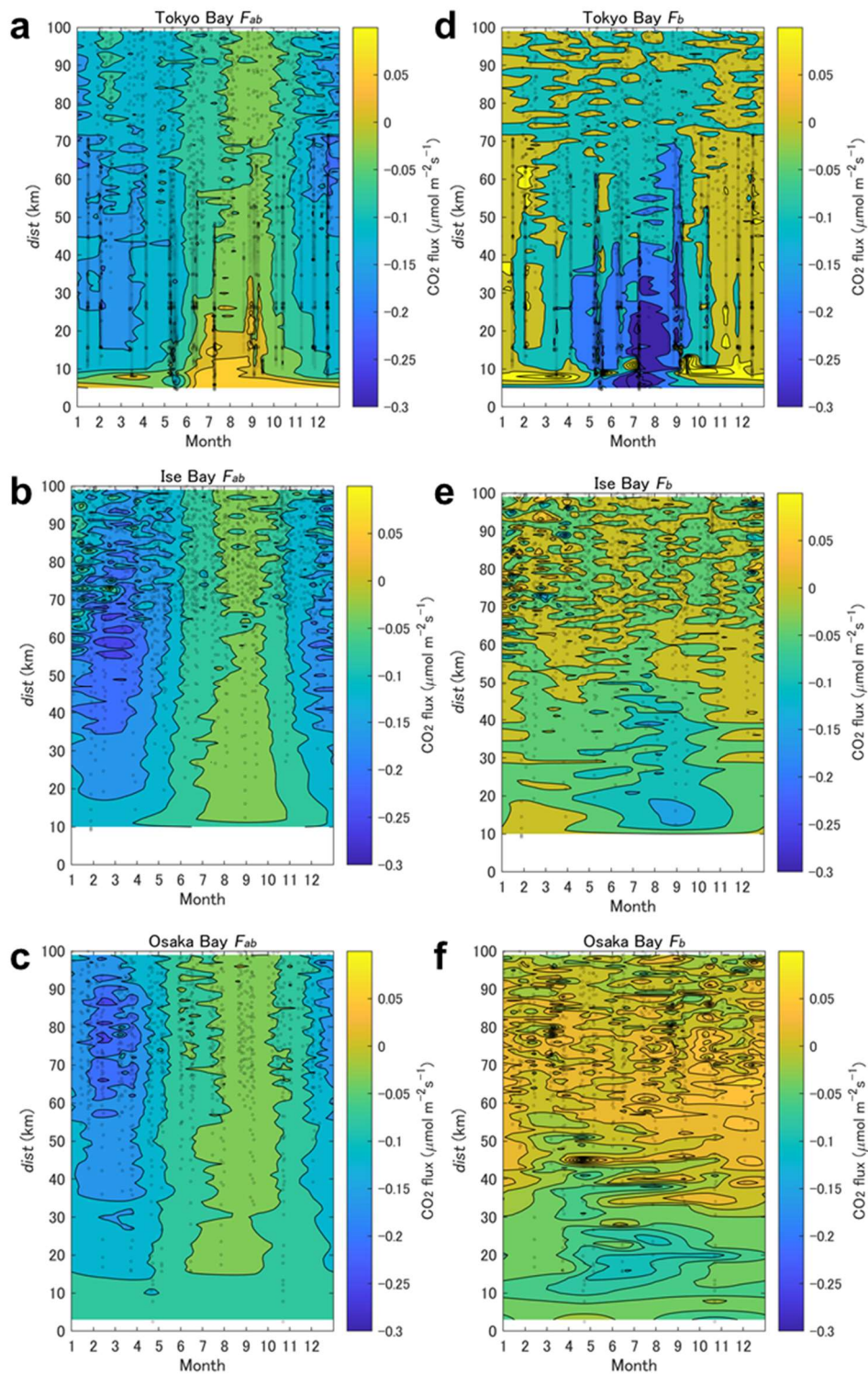


Figure S4. Temporal and spatial distributions of the abiotic (F_{ab}) ((a): Tokyo Bay, (b): Ise Bay, (c): Osaka Bay) and biotic (F_b) ((d): Tokyo Bay, (e): Ise Bay, (f): Osaka Bay) air–sea CO₂ flux. The colors and dots are as defined in Figure S1. The parameter *dist* represents the distance from a zero point in the mouth of the main river feeding the inner bay (equation [1] in the main text).

Table S1 The locations for the wind data provided by the NEDO Offshore Wind System database (NeoWins; http://app10.infoc.nedo.go.jp/Nedo_Webgis/top.html)

<i>Dist</i> ^a (km)	Tokyo Bay		Ise Bay		Osaka Bay	
	Lat (°N)	Long (°E)	Lat (°N)	Long (°E)	Lat (°N)	Long (°E)
0	35.65	139.85	35.04	136.74	34.68	135.41
10	35.565	139.81875	34.970	136.81250	34.585	135.31875
20	35.440	139.76250	34.890	136.76250	34.570	135.18125
30	35.365	139.77500	34.815	136.72500	34.475	135.06875
40	35.270	139.76875	34.700	136.80000	34.345	135.01250
50	35.185	139.78125	34.615	136.90000	34.245	134.97500
60	35.095	139.74375	34.545	137.02500	34.130	134.94375
70	35.005	139.71250	34.445	137.06250	34.030	134.91250
80	34.915	139.71250	34.430	137.27500	33.905	134.92500
90	34.820	139.74375	34.425	137.45625	33.805	134.93750
100	34.735	139.74375	34.525	137.72500	33.705	134.95000

^a*Dist* is the distance from a zero point in each bay located in the mouth of the primary river at the head of the bay (equation [1] in the main text).

Table S2 The constant random (*Rand*) and riverine (*Riv*) errors in each bay for the interpolated data. The riverine error is the value of the overall average for each bay. ‘+200’ or ‘200’ in ‘Error type’ low indicates the random error or change of the parameter for the case with the upper or lower riverine DIC, respectively. *The error for DIC_{ab} was omitted because of the small (<4 μmol kg⁻¹) random error and because it has the same riverine error as DIC_b. **The error for fCO_{2ab} was omitted because it was almost the same as that of fCO_{2b}.

	Error type	Tokyo Bay	Ise Bay	Osaka Bay
fCO ₂ (μatm)	<i>Rand</i>	0.5	0.5	0.5
TA (μmol kg ⁻¹)	<i>Rand</i>	34	21	35
DIC (μmol kg ⁻¹)	<i>Rand</i>	28	18	29
DIC _b (μmol kg ⁻¹)*	<i>Rand</i>	28	18	29
	<i>Riv + 200</i>	-16	-12	-8
	<i>Riv - 200</i>	+16	+12	+8
fCO _{2b} (μatm)**	<i>Rand</i>	52	28	51
	<i>Rand + 200</i>	64	31	51
	<i>Rand - 200</i>	47	27	51
	<i>Riv + 200</i>	-37	-16	-10
	<i>Riv - 200</i>	+24	+13	+9
<i>F</i> (mol m ⁻² yr ⁻¹)	<i>Rand</i>	0.92	0.85	0.77
<i>F_{ab}</i> (mol m ⁻² yr ⁻¹)	<i>Rand</i>	0.89	0.93	0.88
	<i>Rand + 200</i>	0.80	0.85	0.96
	<i>Rand - 200</i>	0.92	1.02	0.029
	<i>Riv + 200</i>	+1.70	+0.64	+0.37
	<i>Riv - 200</i>	-0.90	-0.51	-0.32
<i>F_b</i> (mol m ⁻² yr ⁻¹)	<i>Rand</i>	1.30	1.26	1.19
	<i>Rand + 200</i>	1.25	1.21	1.12
	<i>Rand - 200</i>	1.42	1.33	1.25
	<i>Riv + 200</i>	-1.70	-0.64	-0.37
	<i>Riv - 200</i>	+0.90	+0.51	+0.32

References

Lavielle, M. (2004). Using penalized contrasts for the change-point problem. *INRIA*, inria-00070662.

Millero, F. J. (1979). The thermodynamics of the carbonate system in seawater. *Geochimica et Cosmochimica Acta*, 43(10), 1651–1661. [https://doi: 10.1016/0016-7037\(79\)90184-4](https://doi.org/10.1016/0016-7037(79)90184-4)